Superconductivity and Cryogenics
Vol.11, No.4, (2009), pp.1~7

High-temperature superconductors for NMR/MRI magnets:opportunities and challenges

Yukikazu Iwasa,* Juan Bascuñán, Seungyong Hahn, Weijun Yao

Francis Bitter Magnet Laboratory, Massachusetts Institute of Technology, Cambridge, MA

Received 26 July 2009; accepted 19 October 2009

***Abstract*– The unique features of HTS offer opportunities and challenges to a number of applications. In this paper we focus on NMR and MRI magnets, illustrating them with the NMR/MRI magnets that we are currently and will shortly be engaged: a 1.3 GHz NMR magnet, an "annulus" magnet, and an MgB_2 whole-body MRI magnet. The opportunities with HTS include: 1) high fields (e.g., 1.3 GHz magnet); 2) compactness (annulus magnet); and 3) enhanced stability despite liquid-helium-free operation (MgB_2 whole-body MRI magnet). The challenges include: 1) a large screening current field detrimental to spatial field homogeneity (e.g., 1.3 GHz magnet); 2) uniformity of critical current density (annulus magnet); and 3) superconducting joints (MgB_2 magnet).**

1. INTRODUCTION

A tremendous progress achieved in the past decade and that is continuing today has transformed selected HTS materials into "magnet-grade" conductors, i.e., meet rigorous magnet specifications and are *readily* available from commercial wire manufacturers [1]. We are now at the threshold of a new era in which HTS will be a key player, offering opportunities and challenges to a number of applications in superconductivity, including magnets. In this paper we discuss the opportunities and challenges of HTS that are relevant to NMR and MRI magnets, illustrating them with the NMR/MRI magnet programs at FBML that are ongoing and expected to begin in the very near future.

2. Field and Temperature Ranges

Figure 1 shows upper critical field ($\mu_o H_{c2}$) vs. critical temperature (T_c) plots of HTS (Bi2212, Bi2223, MgB_2, YBCO) and LTS (Nb_3Sn and NbTi). We are classifying MgB_2 (T_c = 39 K) as an HTS. Except perhaps Bi2212, these superconductors are magnet-grade conductors. Note that the greater the $\mu_o H_{c2}$ of a superconductor, generally the greater will be the critical current density of the superconductor, which for magnet applications must be above 100 A/mm^2.

Clearly for generation of magnetic fields above ~25 T, e.g., 30.53 T, which corresponds to a proton frequency of 1.3 GHz, HTS is indispensible. Also as evident from Fig. 1,

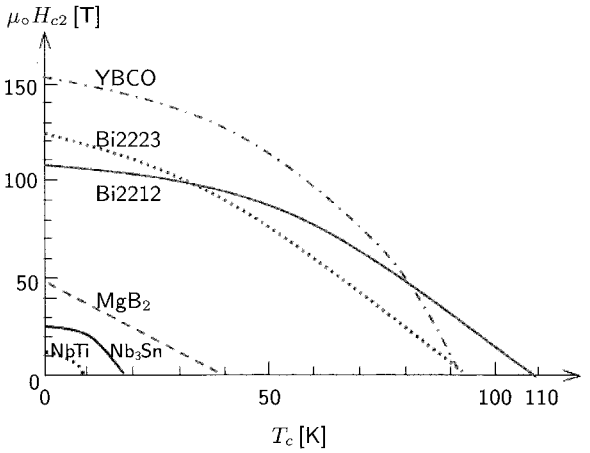

Fig. 1. $\mu_o H_{c2}$ vs. T_c plots for HTS (Bi2212; Bi-2223; MgB_2; YBCO) and LTS (NbTi; Nb_3Sn).

HTS is required for magnet operation above ~10 K, e.g., an MgB_2 MRI magnet operating in the temperature range 10–15 K. That is, Fig. 1 identifies two obvious opportunities offered by HTS: high field and operation above 10 K.

3. Bulk Disk and Thin Plate

Unlike LTS which is now available only as wire, HTS is available not only as wire and tape but also as disk, tube, and even "wide" tape—currently in a width of 40 mm and in the near future 100 mm [2]. YBCO annuli may be manufactured from YBCO disks and plates cut from a wide tape; these annuli may be assembled into a magnet, e.g., a compact "annulus" NMR magnet.

Figure 2a shows a photograph of a YBCO bulk annulus with overall dimensions of 25-mm i.d, 48-mm o.d. (5-mm thick), prepared from a 48-mm diameter bulk disk [3]. Figure 2b shows a schematic drawing of two YBCO square plates cut from a long coated YBCO tape 40-mm wide, each square plate with a 25-mm hole [2]. Bulk annuli, square plates, or a combination of these may be stacked to form a compact "annulus" NMR magnet [4]. In stacking square plates, we may rotate the next plate sequentially in the azimuthal direction, e.g., by an angle of 45°, so that the annulus magnet will have its effective "outer diameter" equal to the diagonal of the square plates.

* Corresponding author: iwasa@jokaku.mit.edu.

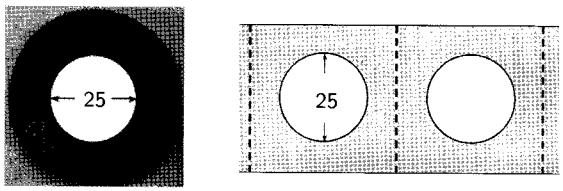

(a) (b)

Fig. 2. (a) Photograph of a YBCO bulk annulus with a 25-mm hole prepared from a 48-mm o.d. YBCO disk [3]. (b) Schematic drawing of plate squares, each 40-mm ×40-mm, with a 25-mm hole at the center, cut from a coated 40-mm wide YBCO tape.

4. OPPORTUNITIES: EXAMPLES

Here, we describe three examples of NMR or MRI magnets being currently developed and will be in the very near future at FBML. Each magnet takes advantage of at least one of the three opportunities offered by HTS.

4.1 HIGH FIELD

As stated above, for a magnet generating a field above ~25 T, HTS is indispensable. One prominent class of above ~25-T magnets is for ≥1-GHz NMR spectroscopies, one example of which is a 1.3 GHz NMR magnet that we are working at the moment.

1.3-GHz LTS/HTS NMR Magnet In 2000 the National Institutes of Health awarded FBML the Phase 1 program of a 3-phase program to complete a 1-GHz NMR magnet comprised of an LTS background field magnet and an HTS insert. Although the goal of Phase 1 was modest (a 350-MHz or 8.22-T magnet) [5], this 3-phase program was the first national project with a specific goal to complete a 1-GHz magnet comprising LTS and HTS magnets. In 2007 the target frequency was raised to 1.3 GHz.

The total cost of a ≥1-GHz LTS/HTS NMR magnet is driven by the cost of a high-field/wide bore LTS NMR magnet. Generally, the lower the field, the lower the cost of such a magnet even though a lower field obviously requires a wider *cold* bore, because the companion HTS insert must be larger to make up for a reduced field contribution of the LTS magnet.

TABLE I
HIGH-FIELD LTS NMR MAGNETS.

Frequency [MHz]	900	900	700	500
Center field [T]	21.11	21.11	16.44	11.74
Operating temperature [K]	1.8	4.2	4.2	4.2
Cold bore [mm]	135	135	236	236
Operating current, I_{op} [A]	248.7	180.6	251.0	250.0
Magnetic energy @I_{op} [MJ]	42.5	103	20.9	4.7

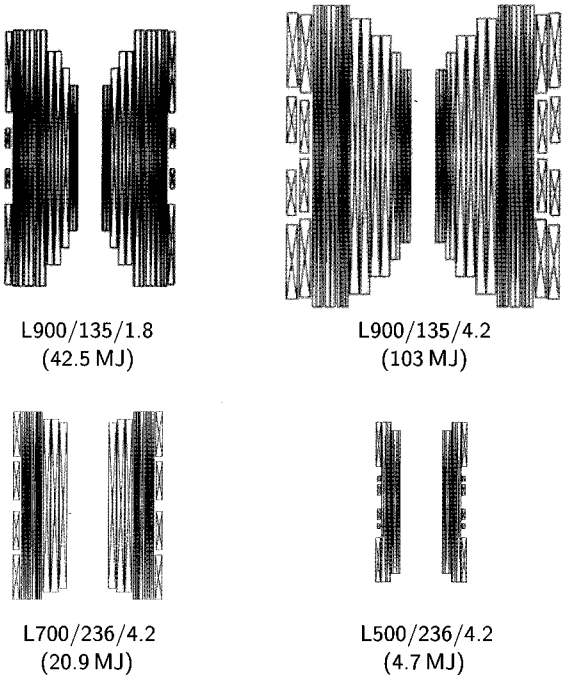

Fig. 3. In-scale cross sectional profiles of 4 LTS magnets, each comprising NbTi and Nb_3Sn coils listed in Table I. The 900-MHz, 700-MHz, and 500-MHz LTS magnets in Table I are designated, respectively, as L900, L700, and L500. The stored magnetic energy for each magnet is given in parentheses.

Table I lists key magnet and operating parameters of four high-field LTS NMR magnets at frequencies of 900 MHz (at 1.8 K and 4.2 K), 700 MHz (4.2 K), and, as a reference, 500 MHz (4.2 K), prepared by JASTEC [6]. Figure 3 presents in-scale cross sectional profiles of the LTS magnets represented in Table I, the 900-MHz (L900), 700-MHz (L700), and 500-MHz (L500) LTS magnets; the L500 is on hand at FBML. The stored magnetic energy for each magnet is given in parentheses.

Note that there are two versions of L900, one operating at 1.8 K and the other at 4.2 K. At 1.8 K the performance of Nb_3Sn coils is superior to those at 4.2 K, particularly at fields above ~19 T, making the 1.8-K L900 substantially more compact than the 4.2-K L900. Below ~17 T the incremental gain in the performance of Nb_3Sn coils is negated by increased system complexity and extra cost associated with operation at 1.8 K. Note also that the gain in HTS performance achieved at sub-4.2 K operation is negligible but its slight resistance, due chiefly to splices and index dissipation, makes 1.8-K operation of an HTS insert more expensive, cryogenically, than 4.2-K operation.

L700/H600 Choice For a 1-GHz LTS/HTS NMR magnet, 900 MHz is the choice for the LTS magnet (L900) by other groups that, after MIT, began working on or planning to build ≥1 GHz LTS/HTS NMR magnets. [7]. This

too was our choice in 1999 at the outset of the 3-phase program. However, because the cost of an LTS magnet increases sharply more with field than bore size, as may be inferred from the magnetic energies of the LTS magnets listed in Table I and indicated in Fig. 3. Therefore, we believe that to reduce the overall cost of a ≥1-GHz LTS/HTS NMR magnet, L900 may not be optimal.

Our choice of the L700/H600 division for a 1.3 GHz magnet is to balance the decreasing cost of an LTS magnet on one hand and increasing technical challenges of an HTS insert on the other. For example, an L700 with a cold bore of 236 mm operating at 4.2 K has a magnetic energy nearly $1/5^{\text{th}}$ that of an L900 with a cold bore of only 135 mm operating at 4.2 K; its cost will likely be less than that of L900 by nearly the same factor. Note also that a cold bore of 135 mm is just sufficient to accommodate an HTS insert generating no greater than 200 MHz, i.e., it is not possible to achieve a field of 1.3 GHz with a 900-MHz LTS magnet, operated at 1.8 K or 4.2 K, having a cold bore of only 135 mm. Such a magnet having a cold bore of 236 mm will likely to have a magnetic energy of >100 MJ (1.8 K) and that approaching 300 MJ (4.2 K).

H600 The 600-MHz HTS insert consists of three nested stacks of double-pancake coils, each wound with HTS tape, YBCO, Bi2223, or even a combination of both. Although a stack of double-pancake coils by itself is not detrimental in generating a spatial field distribution required for a high-resolution NMR magnet, a tape-wound magnet poses a challenge, which is the next topic of this paper.

4.2 COMPACT MAGNET

Whereas the cross sectional area of coated YBCO is almost entirely (~99%) occupied by non-superconducting materials, the opposite is the case with bulk YBCO disk. The engineering critical current density, J_e (= critical current/total conductor cross sectional area) is thus at least one order of magnitude greater for bulk than for coated tape. A large J_e leads to a large overall current density, λJ (= total ampere turns/winding cross sectional area). For a given center field, the greater the λJ, the smaller will be the winding volume. Thus, bulk disks are suitable to build a compact magnet. Table II lists values of superconductor critical current density, J_c, and J_e/J_c for bulk disk and coated tape at selected combinations of temperature and field perpendicular to the conductor surface, $B_\perp$.

TABLE II
CURRENT DENSITIES: BULK & COATED YBCO.

	J_c [A/m^2]	J_e/J_c
Bulk YBCO		
@77 K; $B_\perp$ = 1.1 T	0.3×10^9	≈ 1
@29 K; $B_\perp$ = 17 T [8]	3×10^9	≈ 1
Coated YBCO Tape		
@77 K; self field	25×10^9	≈ 0.01–0.02
@20 K; $B_\perp$ = 5 T	10×10^9	≈ 0.01–0.02

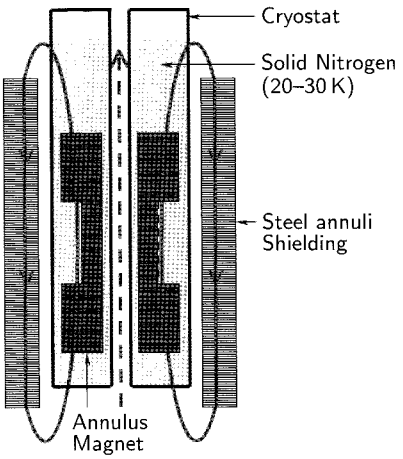

Fig. 4. Schematic drawing of an annulus magnet. The lines represent the trapped magnetic fields. No mechanical, electrical, and cryogenic details, including the primary cooling source, a coldhead of a cryocooler, are shown. The system has an overall diameter typically of ~300 mm.

Annulus Magnet Currently, we are developing a prototype compact "NMR-class" annulus magnet, assembled from bulk YBCO annuli and YBCO plate annuli (see Fig. 2). Such a compact (desktop) NMR magnet will have widespread use in pharmaceutical and food industries in the discovery/development stage. It may also become an in-office tool for the doctor to efficiently and properly evaluate the effects of a drug prescribed to the patient. Figure 4 shows a schematic drawing of an annulus magnet.

System The key components of an annulus magnet include: 1) an annulus magnet, which in operating mode is immersed in solid nitrogen; 2) a cryostat; 3) an energizing electromagnet to "field-cool" the annulus magnet—this energizing magnet must have a room-temperature bore large enough to accommodate the cryostat; 4) a coldhead (not shown in Fig. 4) of a cryocooler, placed at the cryostat top, to keep both the annulus magnet and the solid nitrogen at a nominal operating temperature of 20 K; and 5) steel annulus sheets to reduce the fringing field, added over the cryostat o.d. after the annulus magnet is energized and the cryostat is removed from the energizing magnet.

Prototype The principal aims of the on-going 2-year program are four-fold.

1) Demonstrate the feasibility of trapping strong a magnetic field with YBCO annuli. The prototype annulus magnet will operate in the range 100–150 MHz and have a room-temperature bore of ~10 mm. The dimensions (i.d., o.d., and thickness) of each annulus, and the spacing between adjacent ones, are determined to enable the prototype to generate an NMR-class spatially homogeneous field. After the annulus magnet is energized with an electromagnet, it will be shielded with steel annuli placed outside the cryostat.

2) Demonstrate, with the prototype, the unique feature of the annulus magnet that can be energized at one site

(magnet manufacturer) and transported to another site (user) with no degradation of its NMR-quality field.

3) Demonstrate an innovative "field-tweaking" technique that permits fine-tuning of the current distribution in each annulus and thus the axial field homogeneity.

4) Demonstrate the innovative cryogenic system of a magnet that:

a) keeps, with the cooling source on, the magnet and a volume of solid nitrogen at a nominal operating temperature of 20 K; and

b) enables, with the cooling source disengaged, the energized annulus magnet to maintain its persistent-mode field for a substantial period of time of at least two days, for shipment from the manufacturer's site to the user site.

We believe that successful completion of our prototype annulus magnet would lead to a new type of persistent-mode, high-resolution desk-top NMR magnet, in which compactness, simple manufacturability (therefore, low cost), and ease of operation are key virtues.

4.3 OPERATION AT ≥10-K & STABILITY

The critical temperature (T_c) of MgB_2 ~40 K promises obvious advantages; compare this with those of the low-temperature superconductors (LTS) currently used in all superconducting MRI magnets, ~10 K (NbTi) and ~18 K (Nb_3Sn). Owing to the higher T_c, an MgB_2 magnet will have its stability considerably enhanced and cryogenic system substantially simplified.

Liquid Helium vs. Superconducting Magnets The traditional method to maintain the operating temperature, T_{op}, of an LTS magnet is by its immersion in a bath of liquid helium (LHe), generally at 4.2 K. Recently, a closed cryogenic system has become commercially available in which a cryocooler condenses the effluent helium vapor to maintain the LHe in the cryostat, unnecessitating liquid refill. With the depletion of helium resource, the helium price is expected to double every ~5 years. A helium-free system is becoming more desirable in the future.

LHe-Free Superconducting Magnets Ideally, every superconducting magnet, LTS or HTS, should operate without reliance on LHe. Indeed, LHe-free superconducting magnets have been developed in which the magnet windings are cooled directly by cryocoolers. General Electric (GE) initiated a trend towards such "dry" superconducting MRI magnets in the early 1990s with an all-Nb_3Sn magnet MRI system. Their 0.5-T magnets operated at 10 K, the practical limit of Nb_3Sn. Despite the LHe-free, easy-to-operate features, the production was terminated after only a few years in the market chiefly because the 10-K Nb_3Sn conductor costs ~10 times the 4.2-K NbTi. The GE experience shows that the key to marketplace success, and thus widespread use of dry MRI magnets, is the conductor performance/price ratio whether it is HTS operated at ≥10 K or LTS NbTi at 4.2 K: an MgB_2 magnet with a 10–15 K operating temperature range appears promising.

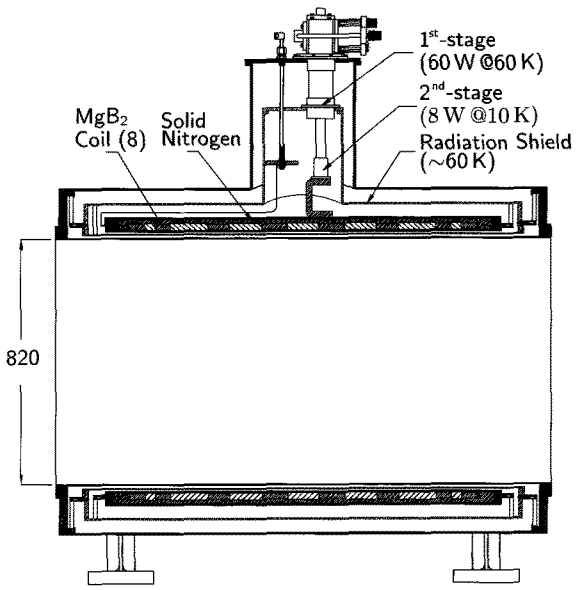

Fig. 5. Fig. 5 In-scale sketch of a 0.5-T/820 mm bore whole-body MRI magnet wound with MgB_2.

Temperature Uniformity Over Winding To ensure thermal stability of a magnet, the temperature throughout the magnet winding must be uniform at its operating point, T_{op}. For NbTi magnets, the tolerance for temperature non-uniformity in most cases is no greater than ~1 K. Such a stringent requirement for temperature is achieved most readily by immersion of an LTS magnet in liquid cryogen. As discussed above in reference to Fig. 1, HTS is required for magnet operation above ~10 K, i.e., $T_{op} \geq 10$ K. A significant advantage of ≥ 10-K operation is that an HTS can function stably over a large operating temperature range, ΔT_{op}, whereas the basic tenet of stability for LTS magnets is $\Delta T_{op} \sim 0$. This large permissible ΔT_{op} makes the operation in dry conditions much easier for HTS magnets than their LTS counterparts [9]

Stability of Adiabatic Magnets Even an adiabatic magnet, i.e., no local cooling, tolerates a small temperature rise, $\Delta T_{op} \leq [\Delta T_{op}]_{mn}$, from T_{op}. The enthalpy energy density required to raise the conductor temperature from T_{op} by $[\Delta T_{op}]_{mn}$ is known as energy density margin, Δe_h. Table III lists approximate values of Δe_h of three types of magnets. Clearly, our MgB_2 magnet, owing to ≥ 10-K operation and a large $[\Delta T_{op}]_{mn}$, is most stable of all.

TABLE III
ENERGY MARGIN—COMPARISON.

T_{op} [K]	$[\Delta T_{op}]_{mn}$ [K]	Δe_h [mJ/cm^3]	Magnet Type
2.3	~0.25	~0.1	500-MHz NMR magnets
4.2	~1	~1	"typical" 5-T NbTi magnets
10	5	~10	MIT MgB_2 MRI magnet

5. CHALLENGES: EXAMPLES

Challenges for HTS magnets include: 1) a large screening current field; 2) uniformity of critical current density; and 3) superconducting splices. These challenges are discussed with our HTS magnet programs as examples.

5.1 SCREENING-CURRENT FIELD (SCF)

Figure 6 shows an NMR signal of our Phase 2 "L600/H100" NMR magnet, comprising a 600-MHz LTS magnet (L600) and a 100-MHz HTS insert (H100) [10, 11]. Its resonance frequency, f_R, is 692.2056551 MHz with a half-width frequency of ~1.5 kHz. This large half-width frequency implies that the Phase 2 magnet is not a high-resolution NMR magnet, which typically has a half-width of ≤ 10 Hz.

It has been determined that the chief source of this poor field quality stems from a screening current field (SCF) or a remanent field, induced in the Bi2223 tape of the H100 [12–15]. An SCF is present in every magnet wound with a Type II superconductor that includes every "magnet-grade" conductor, LTS or HTS. In AC devices this SCF is the source of hysteresis losses.

The SCF is not a design issue with LTS NMR magnets because LTS coils are wound with multifilamentary wire composed of many *twisted* filaments, each less than ~50 μm in diameter. The Bi2223 tape, 4-mm wide, in the H100 is composed of many *untwisted* "mini tapes," each ~500 μm wide embedded in silver matrix. It means the SCF of a Bi2223-tape wound coil can be at least ~10 times and perhaps up to ~100 times greater than that of an LTS coil, and *time-dependent*. Because of this SCF, Bi2223 and YBCO, both available only in tape, are deemed not ideal superconductors for electric power devices.

Remedies There are three possible remedies to eradicate or minimize an SCF of an HTS insert: 1) use of multifilamentary HTS wire similar to LTS wire; 2) twist mini tapes and further reduce their widths; 3) shim the field errors caused by SCF. Of these remedies, the 1st remedy may be achievable when multifilamentary Bi2212 wire becomes a magnet-grade conductor; the 2nd seems an impossible remedy, because, though conductor designs have been proposed to reduce the effective size and decouple mini tapes [— —], such designs are likely not economically feasible; the 3rd appears to be the only practical remedy. For our 1.3 GHz L700/H600 magnet, a set of superconducting shim coils specifically targeted to minimize the error fields generated by the H600 will be installed in the L700.

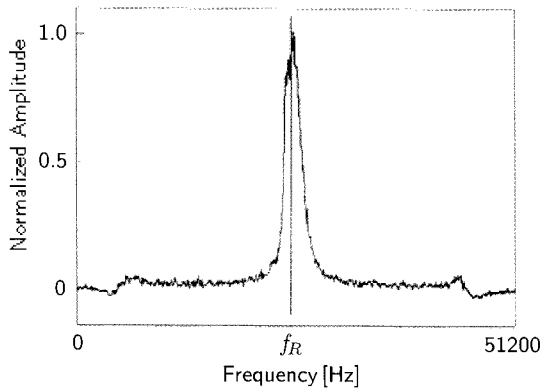

Fig. 6. NMR signal of the Phase 2 L600/H100 magnet at 692.2056551 MHz, with a half-width of ~1.5 kHz.

5.2. J_c UNIFORMITY

Conductor-Wound NMR Magnet With an NMR magnet wound with conductor, the location of each current element within the winding is well-defined by the conductor and winding dimensions. Therefore, *on paper* the magnet can be designed to meet specified field homogeneity requirements; in a *real* magnet winding errors creep in, making it impossible to place every current element exactly at its computed location. Still, the conductor location is usually within an acceptable tolerance; this is true especially with NMR magnets wound with LTS.

Annulus Magnet With a *real* annulus, controlling the location and *magnitude* of every current element is a challenge. Ideally, the induced-current pattern of an annulus should be perfectly symmetric in the azimuthal direction, as schematically drawn in Fig. 7a. However, owing to imperfections and defects introduced during the manufacturing processes, which also affect *local* J_c, an annulus can induce unsymmetric current patterns, one possible example of which is schematically drawn in Fig. 7b.

Symmetric and unsymmetric current patterns observed in real bulk annuli are shown in Fig. 8 [3]. Each set of cur-

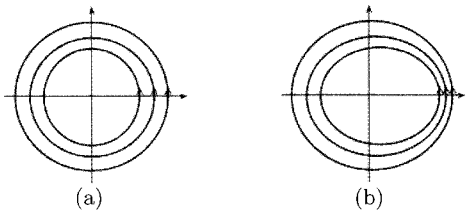

Fig. 7. Schematic drawings of induced critical current contours in the azimuthal direction in a bulk annulus. (a) symmetric; (b) non-symmetric.

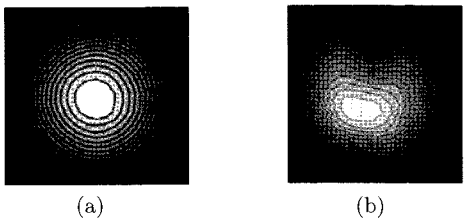

Fig. 8. Induced critical current contours in the azimuthal direction in two bulk annuli, based on measured surface trapped field distribution as each annulus is field-cooled at 77 K. (a) nearly symmetric; (b) non-symmetric.

rent contours is generated from the surface field distribution of an annulus field-cooled at 77 K. The induced current pattern shown in Fig. 8a is nearly symmetric, while that shown in Fig. 8b is not. Thus, for an annulus NMR magnet the first annulus is usable but not the second annulus.

A big challenge for constructing an annulus NMR magnet is thus to prepare enough annuli each having an induced current patter that is nearly symmetric in the azimuthal direction.

5.3. SUPERCONDUCTING SPLICES

NMR and MRI superconducting magnets for research and diagnostic activities, are currently all based on LTS, operate in persistent mode, made possible with superconducting splices. To date, with the exception of MgB_2, techniques have not been developed to make superconducting splices for HTS (Bi2212, Bi2223, coated YBCO), tapes or wires, that are practical in a *coil winding/assembly environment.* Although progress in signal processing techniques has made a persistent-mode field no longer an absolute necessity, still, it is desirable to operate *any* superconducting magnet for NMR or MRI in persistent mode.

Because these techniques often contain proprietary information, even when a successful technique appears to have been developed, technical details are often not reported.

Splice Techniques for Bi2212 & Bi2223 Although the so-called "superconducting" joints between HTS tapes were reported as early as in the 1990s [16–18], splice resistances (at 77 K) are in nano-ohms, not good enough to operate an HTS magnet in persistent mode. Subsequent results have not been satisfactory either, because either resistance is still too large (1 $\mu\Omega$ @4.2 K) [19] or a combination of a large resistance (0.1 $\mu\Omega$ @77 K) and a low current-carrying capacity (~20 A at 77 K in zero field) [18]. Note that for a splice reported in [19], its current-carrying capacity improved from 77 K to 4.2 K but not its resistance. As reported in [20], this splice does not depend on a superconducting solder. If it did, its resistance would have disappeared when operated at 4.2 K.

YBCO As of today no successful technique to join YBCO coated tapes has been reported, though work to develop a technique is undoubtedly taking place now.

MgB_2 The first MgB_2 splice, reported in 2005 by Hitachi [21], involves splicing NbTi wire and MgB_2 tape for an MgB_2 coil operated at 4.2 K in "persistent mode," though measurement resolutions were insufficient to verify that the joints were superconducting. ASG Superconductor in 2006 reported results of their MgB_2-MgB_2 joint, citing a joint resistance ¡$10^{-14}\,\Omega$ [22]. To date neither group has disclosed their splicing techniques. In 2008, Yao of our group succeeded in developing a splicing technique applicable to *unreacted* multifilamentary (18) MgB_2 wires, each 0.84-mm diameter. Figure 9 shows I_c vs. temperature data for a superconducting MgB_2 splice; the insert shows resistance vs. temperature plot of a splice near the critical temperature. At least with unreacted multifilamentary MgB_2 wires, there is a positive result to the challenge to make superconducting splices.

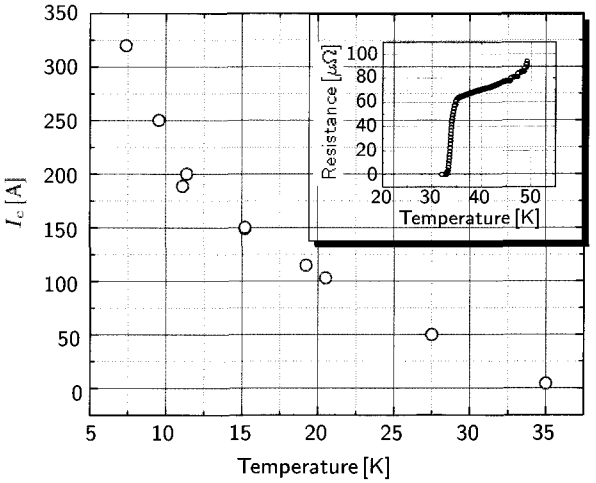

Fig. 9. I_c vs. T data for an MgB_2 splice in self field. Inset: resistance vs. temperature data of the splice, showing the superconducting transition.

6. CONCLUSIONS

In this paper key opportunities that HTS offers to superconducting magnets are first discussed. These include: 1) high fields; 2) compact magnets; and 3) $\geq$10-operation and enhanced stability. The HTS magnet obviously presents technical challenges too. These include: 1) a large screening current field; 2) uniformity of critical current density; and 3) superconducting joint. Both the opportunities and challenges have been discussed with examples drawn from the NMR and MRI projects, all based on HTS, currently on-going or about to start at the Francis Bitter Magnet Laboratory. The on-going programs are completion of: 1) a 1.3 GHz high-resolution NMR magnet comprising an LTS background field (700 MHz) and an HTS insert (600 MHz) and 2) a compact NMR magnet assembled from YBCO annuli. In the next program to be begin shortly, a persistent-mode, liquid-helium-free, fully protected whole-body MRI magnet will be completed, the entire magnet to be wound with multifilamentary MgB_2 wire and operated in the temperature range 10–15 K.

ACKNOWLEDGMENT

The research programs are supported by the National Institutes of Health. In addition, we thank the Railway Technical Research Institute, Tokyo, for supply of bulk YBCO annuli and American Superconductor Corp. for supply of YBCO tape annuli. The authors would also like to express their gratitude to our colleague and dear friend, the late Dr. Emanuel S. Bobrov, for his many years of contribution to the Magnet Technology Division.

REFERENCES

[1] Yukikazu Iwasa, *Case Studies in Superconducting Magnets* (Springer, 2009).

[2] John Voccio (American Superconductor Corp., personal communication, 2008).

[3] Masaru Tomita, (Railway Technical Research Institute, personal communication, 2007).

[4] Yukikazu Iwasa, Seung-yong Hahn, Masaru Tomita, Haigun Lee, Juan Bascuñán, "A 'persistent-mode' magnet comprised of YBCO annuli," *IEEE Trans. Appl. Superconduc.* **15**. 2352 (2005).

[5] Juan Bascuñán, Emanuel Bobrov, Haigun Lee, and Yukikazu Iwasa, "A low- and high-superconducting (LTS/HTS) NMR magnet: design and performance results," *IEEE Trans. Appl. Superconduc.* **13**, 1550 (2003).

[6] Masatoshi Yoshikawa (JASTEC., personal communication, 2006).

[7] T. Kiyoshi, A. Otsuka, S. Choi, S. Matsumoto, K. Zaitsu, T. Hase, M. Hamada, M. Hosono, M. Takahashi, T. Yamazaki, and H. Maeda, "NMR upgrading project towards 1.05 GHz," *IEEE Trans. Appl. Superconduc.* **18**, 860 (2008).

[8] Masaru Tomita and Masato Murakami, "High-temperature superconductor bulk magnets that can trap magnetic fields of over 17 tesla at 29 K," *Nature* **421**, 517 (2003).

[9] Yukikazu Iwasa, "Stability and protection of superconducting magnets—a discussion," *IEEE Trans. Appl. Superconduc.* **15**. 1615 (2005).

[10] S. Hahn, J. Bascuñán, H. Lee, E.S. Bobrov, W. Kim, and Y. Iwasa, "Development of a 700 MHz low-/high-temperature superconductor for nuclear magnetic resonance magnet: Test results and spatial homogeneity improvement," *Rev. Sci. Instrum.* **79**, 026105 (2008).

[11] Seung-yong Hahn, Juan Bascuñán, Haigun Lee, Emanuel S. Bobrov, Wooseok Kim, Min Cheol Ahn, and Yukikazu Iwasa, "Operation and performance analyses of 350 and 700 MHz low-/high-temperature superconductor nuclear magnetic resonance magnets: A march toward operating frequencies above 1 GHz," *J. Appl. Phys.* **105**, 024501 (2009).

[12] L. Kopera, T. Melisek, P. Kovac, and J. Pitel, "The design and performance of a Bi-2223/Ag magnet cooled by a single-stage cryocooler," *Supercond. Sci. Technol.* **18**, 977 (2005).

[13] C. Gu, T. Qu, and Z. Han, "Measurement and calculation of residual magnetic field in a Bi2223/Ag Magnet," *IEEE Trans. Appl. Superconduct.* **17**, 2394 (2007).

[14] Min Cheol Ahn, Tsuyoshi Yagai, Seungyong Hahn, Ryuya Ando, Juan Bascuñán, and Yukikazu Iwasa, "Spatial and temporal variations of a screening current induced magnetic field in a double-pancake HTS insert of an LTS/HTS NMR magnet," *IEEE Tran. Appl. Superconduc.* **19**, 2269 (2009).

[15] Seung-yong Hahn, Min Cheol Ahn, Emanuel Saul Bobrov, Juan Bascuñán, and Yukikazu Iwasa, "An analytical technique to elucidate field impurities from manufacturing uncertainties of a(n) double pancake type HTS insert for high field LTS/HTS NMR magnets," *IEEE Tran. Appl. Superconduc.* **19**, 2281 (2009).

[16] K. Shibutani, T. Egi, S. Hayashi, Y. Fukumoto, I. Shigaki, Y. Masuda, R. Ogawa and Y. Kawate, "Fabrication of superconducting joints for Bi-2212 pancake coils," *IEEE Trans. Appl. Superconduc.* **3**, 935 (1993).

[17] J.E. Tkaczyk, R.H. Arendt, P.J. Bednarczyk, M.F. Garbauskas, B.A. Jones, R.J. Kilmer, K.W. Lay, "Superconducting joints formed between powder-in-tube $Bi_2Sr_2Ca_2Cu_3O_z$/Ag tapes," *IEEE Trans. Appl. Superconduc.* **3**, 946 (1993).

[18] Phillip V. Shoaff, Yusuf Hascicek, Justin Schwartz, and Steven W. Van Sciver, "An investigation of the characterizations and development of HTS joints in BSCCO 2212/Ag composites," *IEEE Trans. Appl. Superconduc.* **7**, 1695 (1997).

[18] Jung Ho Kim, Kyu Tae Kim, Seok Hern Jang, Jinho Joo, Seyong Choi, Wansoo Nah, Hyoungku Kang, Tae Kuk Ko, Hong-Soo Ha, Sang-Soo Oh, Kang-Sik Ryu, and Philip Nash, "Measurement of joint properties of Bi(Pb)-Sr-Ca-Cu-O (2223) tapes by field decay technique," *IEEE Trans. Appl. Superconduc.* **13**, 2992 (2003).

[19] Jung Ho Kim, Bong Ki Ji, Jinho Joo, Cheol-Woong Yang, Wansoo Nah, "Superconducting joint between Bi-Pb-Sr-Ca-Cu-O superconductor tapes," *IEEE Trans. Appl. Superconduc.* **10**, 1182 (2000).

[21] M. Takahashi, K. Tanaka, M. Okada, H. Kitaguchi, and H. Kumakura, "Relaxation of trapped high magnetic field in 100 m-long class MgB_2 solenoid coil in persistent current mode operation," *IEEE Trans. Appl. Superconduc.* **16**, 1431 (2006).

[22] Roberto Penco and Giovanni Grasso, "Recent development of MgB_2-based large scale applications," *IEEE Trans. Appl. Superconduc.* **17**, 2291 (2007).

[23] Weijun Yao, Juan Bascuñán, Seungyong Hahn, and Yukikazu Iwasa, "A superconducting joint technique for MgB_2 round wires," *IEEE Tran. Appl. Superconduc.* **19**, 2261 (2009).